# NATIONAL ADVISORY COMMITTEE FOR AERONAUTICS

TECHNICAL NOTE 4209

## EXPERIMENTAL THERMAL CONDUCTIVITIES OF THE $N_2O_4 \rightleftarrows 2NO_2$ SYSTEM

By Kenneth P. Coffin and Cleveland O'Neal, Jr.

Lewis Flight Propulsion Laboratory
Cleveland, Ohio


Washington
February 1958

NATIONAL ADVISORY COMMITTEE FOR AERONAUTICS

TECHNICAL NOTE 4209

# EXPERIMENTAL THERMAL CONDUCTIVITIES OF THE $N_2O_4 \rightleftharpoons 2NO_2$ SYSTEM

By Kenneth P. Coffin and Cleveland O'Neal, Jr.



## SUMMARY

The thermal conductivity of reacting gas systems has been treated theoretically by various investigators; but reliable, direct measurements of the thermal conductivity of reacting systems for which satisfactory calculations can be made are not available. This investigation was designed to supply the needed data.

The thermal conductivity of the $N_2O_4 \rightleftharpoons 2NO_2$ system was measured by a hot-wire technique at temperatures between 20° and 215° C and pressures from 1/3 to 1 atmosphere; approximate values were obtained at pressures as low as 0.02 atmosphere from 20° to 80° C. The experimental values for the equilibrium system were found to be as much as nine times those computed for the equivalent nonreacting system.

Excellent agreement was obtained between the experimental values for the equilibrium thermal conductivity of the $N_2O_4 \rightleftharpoons 2NO_2$ system and the calculated values. Minor discrepancies did occur, and explanations for these are suggested.

## INTRODUCTION

The problems of heat transfer in chemically reacting gases have become increasingly important; dissociating gas systems exist in the exhaust nozzles of jet engines and within the boundary layer on hypersonic aircraft. References 1 and 2 consider heat transfer in such systems and, in this respect, the thermal conductivity of reacting gas mixtures is quite important. In this report, the thermal conductivity is considered to include the effects of the chemical enthalpy associated with the dissociation as well as the internal energy normally associated with an Eucken-type correction.

Interest in the thermal conductivity of dissociating gases is not new. The problem was treated theoretically soon after the turn of the century (ref. 3) and again at the quarter-century mark (ref. 4). Recently, the subject has been developed further to include general gaseous reactions

(refs. 5 and 6). Such papers conclude that the thermal conductivities of dissociating gases (a special case of reacting gases) in chemical equilibrium should be an order of magnitude greater than in the equivalent "frozen" mixture.

Specifically, reference 6 considers the $N_2O_4 \rightleftarrows 2NO_2$ and the $(HF)_6 \rightleftarrows 6HF$ systems; the theoretical expressions were used to compute values that were compared with the existing data. For the $(HF)_6 \rightleftarrows 6HF$ system, the data of reference 7 are in good agreement with the calculated values; however, the exact nature of the dissociation is not clear, and the estimation of the force constants for the calculation is rather uncertain. For the $N_2O_4 \rightleftarrows 2NO_2$ system, the values of conductivity were deduced (ref. 3) from heat-transfer measurements (refs. 8 and 9) and supported the theory only qualitatively.

Because of the general interest in, and the significance of, the applications of the theory, direct measurements of the thermal conductivity of the $N_2O_4 \rightleftarrows 2NO_2$ system have been made. By using a hot-wire technique, relative values of thermal conductivity were obtained from room temperature ($20^\circ$ C) to $215^\circ$ C over a pressure range of 1/3 to 1 atmosphere. Some additional values were obtained at pressures as low as 0.02 atmosphere in the temperature range $20^\circ$ to $80^\circ$ C. Thermal conductivity is independent of pressure in a nonreacting system; however, in the dissociating system the effect of pressure is a change in composition, which results in a pressure dependence in the conductivity of the system.

Calculated values of the frozen and equilibrium thermal conductivities are presented for the temperature and pressure ranges covered by the experiments. These computed values are compared with the experimental values; to some extent the agreement is controlled by the selection of the force constants for the calculations. Explanations are proposed for minor deviations.

## APPARATUS AND PROCEDURE

### Apparatus

Thermal conductivity cells. - The various designs of hot-wire thermal conductivity cells have been discussed widely (refs. 10 to 13). The design used in this investigation is shown in figure 1. The significant features are the physical characteristics of the cells and the high degree of symmetry throughout the construction. All other dimensions and design features are arbitrary and, in principle, do not affect the performance of the device.

A stainless-steel block, 7 by $3\frac{1}{8}$ by 2 inches, contains four cells symmetrically located for uniformity in cell-wall temperature. At both ends of each pair of cells are caps $1\frac{3}{8}$ inches high and $2\frac{5}{8}$ inches in diameter; they are sealed to the block with stainless steel O-rings. The long leads to the exterior are 0.020-inch platinum wires in two-hole alumina tubing swaged in 1/8-inch stainless-steel tubing. The leads, as well as the 3/8-inch gas inlets, are held to the caps by torqueless "Swagelok" fittings. The gas inlets, one for each pair of cells, lead to both the top and bottom caps.

The 0.005-inch-diameter platinum filaments are alined in the 2-inch-long, 3/16-inch-diameter cells by sapphire watch jewels; the jewels are mounted in small plates closing each end of the cell (the bottom jewel plates are perforated for purging the cells; the top jewel plates are solid to prevent convection into the upper caps). The wire itself is suspended by the weld bead above the upper jewel; it is kept taut by a small weight in the lower cap and by spring tension in the bottom leads. Within the caps the wire leads above the weld at the upper jewel and below the weld just under the lower jewel are not a part of the filament electrically, but are a part of the external lead resistance.

Electric circuits. - The following is a simplified schematic drawing of the instrument:

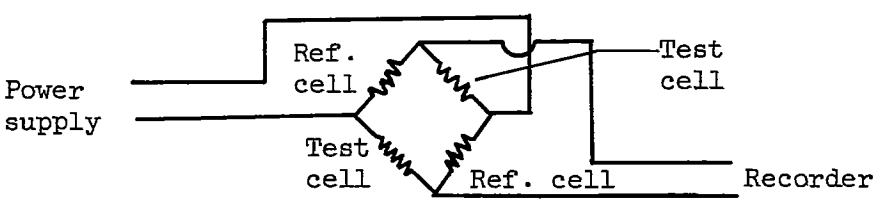


The two pairs of cells (one pair, reference; one pair, test) were connected as the elements of a Wheatstone bridge in an arrangement (ref. 14) minimizing the effect of the relatively large lead resistances. The use of pairs of cells, rather than single cells, doubles the sensitivity of the instrument and produces only a slight increase in complexity. A power supply furnished a well-regulated and monitored 0.5-ampere current to the bridge. The bridge output was recorded on the X-axis of an X-Y recorder.

Oil bath and vacuum system. - The entire cell and cap assembly was immersed in a well-stirred, 8-gallon, mineral-oil bath. The bath was

heavily insulated and fitted with a temperature regulator and five 1250-watt heaters for rapid heating. A copper cooling coil was included to permit rapid cooling or the introduction of a small heat leak. A thermocouple at the center of the block indicated temperature on the Y-axis of the recorder.

The upper ends of the two gas-inlet tubes were butted to glass tubing and closed with short pieces of Tygon tubing (exposed area less than 1/8 sq in.). The glass tubing was sealed into a vacuum system (with an efficient mechanical pump), permitting independent control of the gas in either pair of cells. Under heating conditions, gas pressure in the test cells was maintained constant at 1 atmosphere by a mercury bubbler and at reduced pressures by a Cartesian manostat. Gas pressures were measured with absolute mercury manometers (regularly calibrated against a barometer to correct for contamination by reaction products).

Gases. - Commercial $N_2O_4$ was purified by distillation in the vacuum system. Before each run the $N_2O_4$ was treated with an excess of oxygen to remove traces of impurity (possibly resulting from contact with mercury during the previous run); residual oxygen was pumped off the $N_2O_4$ from a dry ice - acetone bath.

Other gases were used for calibrating the instrument. The neon obtained was reagent grade (>99.5%), while helium (>99.99%), argon (>99.99%), and oil-pumped nitrogen (>99.5%) were stock items.

## Procedure

In general, warmup times of 45 minutes were allowed for all the electrical equipment, including the wires in the cells every time they were shut off. The temperature scale of the Y-axis of this particular recorder was set by a thermocouple in good thermal contact with a thermometer. The reference cells were filled with nitrogen to equal 1 atmosphere at 215° C and were left undisturbed. For the calibrating gases, the test cells were purged repeatedly to change gas; for $N_2O_4$, the test cells were evacuated thoroughly, and $N_2O_4$ was introduced over cold filaments without purging. The heated filaments were exposed only to partial vacuum (2 mm) because of the possibility of burning out the thin wires. The cells were filled rapidly, and no subsequent flow of gas into the cells occurred during any run; in the case of $N_2O_4$, this procedure decreased the chance of contamination of the gas in the cells by products of possible reactions with mercury, Tygon, and stopcock grease.

Varying temperature. - In order to scan thermal conductivity as a function of temperature, the bath was brought to room temperature, and the block was permitted to reach equilibrium. A gas was introduced into

the test cells, and any remaining warmup time was completed. All heaters were turned on, and either the bubbler or the manostat was used to avoid a pressure rise due to gas expansion in the test cells. A time of 62 minutes was required to raise the temperature at the center of the block from 21° to 210° C. During such a run, periodic checks and minor adjustments (if required) were made on the bridge current and on the standardization of the recorder.

Constant temperature. - To eliminate certain erratic low-temperature results attributed to initial transient gradients in the block, as well as to verify the functioning of the instrument, a series of runs was made at constant temperature. The bath and block were brought to the desired temperature, and a small heater was adjusted to compensate for the heat leak (a slight but steady temperature drift was apparently less disturbing to the instrument than a cyclical variation imposed by a regulator). The $N_2O_4$ was introduced and warmup was completed. Then a series of instrument readings was made during a stepwise reduction of the pressure. Immediately thereafter, without cooling the filaments, the cells were purged with helium and nitrogen; 1-atmosphere calibration points were obtained for both gases. All readings for a run were completed in about 20 minutes.



## REDUCTION OF DATA

### Theory of Calibration

The instrument was calibrated by measuring the thermal conductivities of several gases covering the experimental range. This calibration is best understood by considering the theoretical relation between the instrument reading and the thermal conductivity. Very simply, this instrument is a Wheatstone bridge that compares the resistances (temperatures) of two pairs of electrically heated wires, one in the test gas and one in the reference gas. For identical cells, the temperature rise of each wire relative to the temperature of the block is approximately inversely proportional to the thermal conductivity of the gas (ref. 10, p. 11). With gas of thermal conductivity $\lambda_r$ as reference gas, and gas of conductivity $\lambda_t$ as test gas, the wires attain temperatures $T_b + a/\lambda_r$ and $T_b + a/\lambda_t$, respectively, where $T_b$ is the temperature of the block and $a$ is a constant involving the geometry of the cells and the power dissipated by the wire. Therefore, in a bridge circuit, the potential output of the instrument is proportional to the temperature (resistance) difference between the pairs of wires.

$$X_t = a\left(\frac{1}{\lambda_r} - \frac{1}{\lambda_t}\right) + B \qquad (1)$$

where $X_t$ is the reading in millivolts on the X-axis of the recorder and $B$ is a correction for any inherent unbalance of the bridge.

In particular, if the test cells and the reference cells contain the same gas,

$$X_r = a\left(\frac{1}{\lambda_r} - \frac{1}{\lambda_r}\right) + B = B \qquad (2)$$

Moreover, because the thermal conductivities of nonreacting gases have similar dependence upon temperature,

$$X_t \cong \text{constant} + B \qquad (3)$$

for the gas $t$ in the test cells relative to a fixed reference gas $r$. Should $B$ be temperature dependent for any reason, the relation

$$X_t - X_r \cong \text{constant} + B - B = \text{constant} \qquad (4)$$

which follows from equations (2) and (3), should remain valid. Therefore, the recorded curves of bridge output against temperature should be essentially parallel for nonreacting gases.

Further, if the gas in the reference cells remains unchanged ($\lambda_r$ = constant), it is not necessary even to know the identity of the reference gas (in this case, actually nitrogen); and equation (1) assumes the straight-line form

$$X_t = A + \frac{a}{\lambda_t} \qquad (5)$$

At a specified temperature, a plot of $X_t$ against $1/\lambda_t$ for gases of known thermal conductivity should produce a straight-line calibration curve. This calibration curve may then be used to determine the thermal conductivity of an unknown gas.

## Experimental Traces and Sample Calibration Curves

Figure 2 shows a facsimile of the traces obtained during varying-temperature runs. The traces for helium, neon, nitrogen, and argon are essentially parallel; this corresponds to the condition $X_t - X_r \cong$ constant of equation (4). This parallel condition applies even in the low-temperature region, where a pronounced hook appears at the bottom of each curve. The general appearance of the $N_2O_4 \rightleftarrows 2NO_2$ trace is quite distinctive.

A family of calibration curves such as those indicated by equation (5) appears in figure 3. In the figure, values of $X$ have been adjusted by an arbitrary constant at each temperature to prevent the lines from

superimposing. The calibration lines are indeed straight with the exception of the points for argon. This deviation from straightness, when expressed in terms of the thermal conductivity of argon, is within the experimental error. The values of thermal conductivity used for the calibrating gases were obtained from smooth plots of $\lambda$ against T. The plots for helium, neon, and argon were made from the data of reference 15, page 573; for nitrogen the experimental values reported in reference 16 were used.

4753

The system of calibration described should eliminate both physical and electrical effects produced by conditions outside the cells, as well as many minor effects within the cells. The notable exception is the possibility of nonreproducible temperature gradients within the block; in this respect, the symmetry of the cell arrangement and the reproducibility of the heating rate are significant. The calibration curves shown in figure 3 were obtained by averaging, for each of the four gases, two entirely separate traces such as those shown in figure 2. The differences between duplicate traces were normally less than 0.05 millivolt and were frequently no more than 0.01 millivolt, which represents the precision of any single reading (full-scale reading, 0 to 10 mv); such random discrepancies would have little effect on the calibration curves. The general precision of the calibration was such that, in work subsequent to the original detailed calibration indicated here, neon was omitted as a calibrating gas, and single traces were used. As indicated under the constant-temperature procedure, calibration points were taken for helium and nitrogen only; these points were used to construct calibration curves in precisely the same way. These points were also subjected to an additional test which required that they conform to a smooth plot of X against T constructed from the points for all constant-temperature runs.

Although the traces indicated in figure 2 produced satisfactory calibration curves, the thermal-conductivity data from the varying-temperature runs contained minor erratic features in the temperature region below 60° C. These features, together with the rather disturbing and entirely unpredicted hooks at the bottom of the traces, caused some concern about the validity of results from the nonlinear portions of the traces. The nonlinearity is readily attributable to transient gradients occurring within the block while steady-state gradients are being established between the bath and block and within the block. For this reason, the constant-temperature runs were made (as an alternative to reducing the initial temperature of the varying-temperature runs well below room temperature) and have been used in the temperature range below 60° C in place of the results obtained from the dashed-line traces in figure 2.

### Temperature Corrections

A temperature correction was required for varying-temperature runs because the thermocouple used to measure the temperature of the block was located at the center of the block. Obviously, in the case of varying-temperature runs, the temperature at the thermocouple was below that of the cell walls. To determine this correction, a circuit was arranged to use the filaments as resistance thermometers. Then, with helium (high thermal conductivity) in the cells, a simulated varying-temperature run was made to measure filament resistance as a function of thermocouple temperature. Starting from equilibrium, the filaments heated more rapidly than the thermocouple and finally reached a steady-state difference of about $5\frac{1}{2}^{\circ}$ C at and above $50^{\circ}$ C. Accordingly, the $5\frac{1}{2}^{\circ}$ C correction has been applied to the data of varying-temperature runs reported herein.

The magnitude of the temperature gradient between the wire and the cell wall is of particular significance because of the strong dependence of the equilibrium on temperature. From the characteristics of the cells and the wattage produced by the 0.5-ampere current, a rough calculation indicates that $\lambda\Delta T$ is approximately $63\times10^{-5}$ calories per centimeter per second where $\Delta T$ is the temperature difference between the wire and the cell wall. This means that $\Delta T$ is less than $2^{\circ}$ C for the largest values of $\lambda$ observed and as large as $8^{\circ}$ C for the smallest values. The temperatures reported here are cell-wall temperatures.

## RESULTS AND DISCUSSION

### Calculations

One of the major objectives of this investigation was the obtaining of experimental data to verify the predicted increase of thermal conductivity in a dissociating (reacting) system. Therefore, the details of predicting the thermal conductivity are significant. The equation for the equilibrium thermal conductivity $\lambda_e$ appears in reference 6:

$$\lambda_e = \lambda_f + \frac{DP}{RT}\frac{\Delta H^2}{RT^2}\frac{x_1 x_2}{(1 + x_1)^2} = \lambda_f + \lambda_R \qquad (6)$$

where $\lambda_f$ is the "frozen" conductivity (conductivity of a system of equilibrium composition not undergoing any reaction, that is, with a reaction rate equal to zero), and $\lambda_R$ is the contribution to the thermal conductivity due to the chemical reaction (assuming reaction rates sufficiently fast to maintain local equilibrium), D is the binary diffusion coefficient

for the mixture, P is the absolute pressure, T is the absolute temperature, R is the universal gas constant in appropriate units, $\Delta H$ is the heat of reaction, and $x_1$ and $x_2$ are the mole fractions of the undissociated and dissociated materials, respectively. The frozen conductivity $\lambda_f$ has been calculated according to the mixture rules of reference 15 and incorporates the form of the Eucken correction appearing in reference 17; D has been calculated according to reference 15. The force constants $\sigma$ and $\varepsilon/k$ are given in the following table:

| | $\sigma$, Å | $\varepsilon/k$, °K |
|---|---|---|
| $N_2O_4$ | 4.74 | 383 |
| $NO_2$ | 3.90 | 230 |
| $N_2O_4$ - $NO_2$ | 4.32 | 297 |

The selection of the force constants is discussed in reference 18. The heat of reaction and the equilibrium constants (for calculating $x_1$ and $x_2$) were those used in reference 6.

The calculations were performed by IBM techniques at 10° intervals over the temperature range 290° to 490° K for pressures of 1.0, 0.74, 0.5, 0.33, and 0.2 atmosphere and over the range 290° to 420° K for 0.1, 0.05, and 0.02 atmosphere. Values of thermal conductivities for temperatures other than those computed by machine were obtained by interpolating $\lambda_f$ and $(DP/RT)(\Delta H^2/RT^2)$, both slowly varying functions of T obtained from the machine computation, and by computing $x_1$ and $x_2$ for the appropriate P and T. The results of the calculation appear in table I.

It should be emphasized that the detailed agreement between theoretical curves and the experimental data is controlled to some extent by the selection of the force constants and the thermodynamic quantities incorporated in the calculations.

The significant dependence of these calculations on the assumed quantities is of interest with respect to the possibility of changes in the values of the following quantities:

(1) Molecular diameter $\sigma$: $\lambda_e \propto \frac{1}{\sigma_{NO_2}^2}$ provided the ratio $\sigma_{N_2O_4}/\sigma_{NO_2}$ is kept constant; this affects the magnitude of $\lambda_e$.

(2) Equilibrium constant K: $(\lambda_e - \lambda_f) \Big/ \frac{DP}{RT} \frac{\Delta H^2}{RT^2} = \frac{x_1 x_2}{(1 + x_1)^2} = F(K,P)$

because $\lambda_f$ is only slightly dependent upon $x_1$ and $x_2$; this principally affects the temperature at which the maximum value of $\lambda_e$ occurs at given pressure.

(3) Force constant $\varepsilon/k$: Changing $\varepsilon/k$ is equivalent to multiplying by a slowly varying function of T, which is near unity for small changes; it has some effect on both the magnitude and temperature of the maximum value of $\lambda_e$.

## Comparison of Calculation and Experiment

Figure 4 shows data from typical constant-temperature runs. Each run is compared with the theoretical curve corresponding to the experimental temperature. The data much below 1/3 atmosphere are not considered reliable because of possible accommodation effects and the pressure dependence of the instrument observed with calibrating gases below 1/3 atmosphere; these data are included only because of possible interest in the absence of more satisfactory data.

Figure 5 presents the thermal conductivity as a function of temperature for pressures of 1.0, 0.74, and 0.33 atmosphere. The solid line represents the equilibrium thermal conductivity computed as described at the beginning of this section; the dashed line represents the corresponding frozen conductivity. The maximum values of the experimental conductivities are an order of magnitude greater than those calculated for the frozen condition. The data obtained in the temperature range of 20° to 60° C by the varying-temperature method have been replaced by points taken from the constant-temperature curves. As discussed in the REDUCTION OF DATA section, the data eliminated were believed to be less reliable because of the presence of transient gradients. In the temperature range 60° to 80° C, both types of data are included in order to indicate the general agreement obtained by the two methods.

The only major discrepancy within the data appears in the 0.74-atmosphere curve at 60° and 65° C (fig. 5(b)); indeed, it was to some extent the peculiarity of the 0.74-atmosphere results that prompted the use of the constant-temperature method. Because the constant-temperature results proved satisfactory, the extent of experimental deficiencies in the 20° to 60° C range (the transient range) of the varying-temperature method was never established.

On the 1-atmosphere curve (fig. 5(a)), the varying-temperature points marked first series resulted from $N_2O_4 \rightleftarrows 2NO_2$ runs made in connection with the careful calibration described in the REDUCTION OF DATA section. The second series at 1 atmosphere, as well as the data at 0.74 and 0.33 atmosphere, was obtained later. The relatively good agreement of the two entirely different varying-temperature runs (including different calibration curves) tends to support the validity of the varying-temperature method, including the calibration procedure.



The maximums of the data in figure 5 agree quite well with the calculation. While there are minor variations in the maximum values of the equilibrium thermal conductivity (which will be discussed in detail), the positions of the peaks, temperature-wise, are in excellent agreement with theory, with only a minor deviation on the 0.33-atmosphere curve. The over-all agreement in figure 5 between the experimental data and the calculated curves constitutes essential verification of the theory. Nonetheless, there are a few points of discrepancy between the experimental results and the calculated curves that appear to exceed the experimental precision of the results.



## Deviations Between Calculation and Experiment

At the upper end of the experimental range, beginning above perhaps 150° C, $NO_2$ begins to dissociate and a second and even larger maximum might be expected at about 375° C. Experimentally, only the slightest suggestion of a distinct increase in $\lambda_e$ relative to the computed values of $\lambda_f$ exists. Clearly, the calculated curves do not include a contribution for the $NO_2$ dissociation, but the effect should appear experimentally. The logical conclusion is that the reaction rates for the dissociation of $NO_2$ are too slow to be detected by the instrument; that is, in the 3/16-inch cells the diffusion rate is large compared with the rates of reaction. In the temperature region above 175° C, the measured thermal conductivity is that of nearly completely dissociated $N_2O_4$, apparently without the beginning of the dissociation of $NO_2$ into NO and $O_2$. There is, therefore, a possibility that, because the experimental data have values slightly greater than the values calculated, the force constants for $NO_2$ should be modified. However, until the dissociation of $NO_2$ is shown to be completely absent, any attempt to obtain force constants from these data on the assumption of pure $NO_2$ is unwarranted.

In the temperature regions near room temperature, particularly on the 1.00- and 0.74-atmosphere curves (figs. 5(a) and (b), respectively) the experimental values of $\lambda_e$ are somewhat higher than the computed values. The dewpoints of $N_2O_4$ at 1.0, 0.74, and 0.33 atmosphere are approximately

21.0°, 14.7°, and -1.0° C, respectively. The possibility exists that these departures may be caused by gas imperfections arising under conditions of incipient condensation.

Finally, in the relative conductivities there is a definite trend with pressure between the experimental and calculated values of the maximum of $\lambda_e$ in figure 5 (that is, for 1.0 atm, exp. > calc.; for 0.74 atm, exp. ≅ calc.; and, for 0.33 atm, exp. < calc.). In considering the calculation, because $\lambda_f$ is nearly constant over the range of temperature and pressure involved, any variation of $\lambda_e$ must be attributed to $\lambda_R$. Further, because the factor $x_1x_2/(1 + x_1)^2$ is constant (0.125) at the maximum value, the variation of the maximum value of $\lambda_R$ with temperature and pressure must be due to the factor $(DP/RT)(\Delta H^2/RT^2)$. Because the quantity DP is independent of pressure, the apparent pressure dependence of $\lambda_R$ is due, in theory, to the temperature dependence of $(DP/RT)\cdot(\Delta H^2/RT^2)$, which is about $T^{-1.1}$ in the temperature range of 40° to 60° C. However, in the case of the constant-temperature curves of figure 4, similar relative behavior of conductivity with pressure (exp. > calc. at 1 atm; exp. < calc. at 0.33) is observed for the experimental and calculated values.

There is no experimental evidence whatever, in spite of repeated checking, for any pressure dependence of the instrument in the cases of the calibrating gases in the pressure range of 1/3 to 1.0 atmosphere. Further, attributing these effects for $N_2O_4$ to gas imperfections due to condensation would appear difficult because the temperatures of the peaks are considerably above the dewpoint; however, other gas imperfections may be present. The possibility exists that accommodation effects are appearing at unexpectedly high pressure. There may also be exceptional convection effects arising from the unusually high coefficient of expansion for the reacting system.

Nonetheless, a measure of support for the validity of the experimental observations in this matter of deviation with pressure is found in an examination of the $(HF)_6 \rightleftharpoons 6HF$ system reported in reference 7 and analyzed in reference 6. Although no particular significance has been attached previously to the deviations in the case of $(HF)_6$ between calculation and experiment, pressure-wise the deviations have a trend similar to those observed in this investigation.

## SUMMARY OF RESULTS

Equilibrium values of the thermal conductivity of the reacting $N_2O_4 \rightleftharpoons 2NO_2$ system have been measured over a temperature range of 20° to

215° C at pressures of 1.0, 0.74, and 0.33 atmosphere with a hot-wire apparatus calibrated with inert gases of known conductivity. The following results were obtained:

1. At the maximum, equilibrium values of the $N_2O_4 \rightleftarrows 2NO_2$ conductivity are nine times those predicted for the frozen (nonreacting) system.

2. Equilibrium values of the $N_2O_4 \rightleftarrows 2NO_2$ conductivity determined experimentally are in excellent agreement with values calculated by using experimental values of the equilibrium constant and reasonable estimates of the force constants.

3. This investigation, together with the trends observed for the $(HF)_6 \rightleftarrows 6HF$ system, essentially confirms the theoretical predictions of the thermal conductivity of dissociating (reacting) gases in chemical equilibrium.

Lewis Flight Propulsion Laboratory
National Advisory Committee for Aeronautics
Cleveland, Ohio, December 3, 1957

REFERENCES

1. Altman, D., and Wise, H.: Effect of Chemical Reactions in the Boundary Layer on Convective Heat Transfer. Jet. Prop., vol. 26, no. 4, Apr. 1956, pp. 256-258; 269.

2. Fay, J. A., Riddell, F. R., and Kemp, N. H.: Stagnation Point Heat Transfer in Dissociated Air Flow. Jet Prop., vol. 27, no. 6, June 1957, pp. 672-674.

3. Nernst, W.: Chemisches Gleichgewicht und Temperaturgefälle. Festschrift Ludwig Boltzmann Gewidmet, 1904, pp. 904-915.

4. Dirac, P. A. M.: Dissociation Under a Temperature Gradient. Proc. Cambridge Phil. Soc., vol. 22, May 1924, pp. 132-137.

5. Hirschfelder, Joseph O.: Heat Transfer in Chemically Reacting Mixtures, I. Jour. Chem. Phys., vol. 26, no. 2, Feb. 1957, pp. 274-281.

6. Butler, J. N., and Brokaw, R. S.: Thermal Conductivity of Gas Mixtures in Chemical Equilibrium. Jour. Chem. Phys., vol. 26, no. 6, June 1957, pp. 1636-1643.

7. Franck, E. U., and Spalthoff, W.: Das abnorme Wärmeleitvermögen gasförmigen Fluorwasserstoffs. Die Naturwissenschaften, Bd. 40, Sept. 1953. p. 580.

8. Magnanini, G., and Zunino, V.: Sopra il Comportamento Della Conducibilita Termica Dei Vapori Rossi in Rispetto a Variazioni di Temperatura e di Pressione. Gazzetta Chem. Italiana, t. 30, no. 1, 1900, pp. 405-435.

9. Feliciani, C.: Über die Wärmeleitfahigkeit des Stickstoffdioxyds sowie einige Bemerkungen zu einer Arbeit des Herrn Nernst. Phys. Zs., Jahrg. 6, no. 1, Jan. 1905, pp. 20-22.

10. Daynes, H. A.: Gas Analysis by Measurement of Thermal Conductivity. The Univ. Press (Cambridge), 1933.

11. Gregory, H. S.: The Effect of Temperature on the Thermal Conductivity and the Accommodation Coefficient of Hydrogen. Proc. Roy. Soc. (London), ser. A, vol. 149, no. A 866, Mar. 1935, pp. 35-56.

12. Archer, C. T.: Thermal Conduction in Hydrogen-Deuterium Mixtures. Proc. Roy. Soc. (London), ser. A, vol. 165, no. A 923, Apr. 27, 1938, pp. 474-485.

13. Kannuluik, W. G., and Law, P. G.: The Thermal Conductivity of Carbon Dioxide Between 78.50° C and 100° C. Proc. Roy. Soc. Victoria, vol. 58 (N.S.), pts. I-II, 1947, pp. 142-156.

14. Warshawsky, Isidore: A Multiple Bridge for Elimination of Contact-Resistance Errors in Resistance Strain-Gage Measurements. NACA TN 1031, 1946.

15. Hirschfelder, Joseph O., Curtiss, Charles F., and Bird, R. Byron: Molecular Theory of Gases and Liquids. John Wiley & Sons, Inc., 1954. (Especially ch. 8.)

16. Hilsenrath, Joseph, et al.: Tables of Thermal Properties of Gases. Cir. 564, NBS, Nov. 1, 1955.

17. Hirschfelder, Joseph O.: Heat Conductivity in Polyatomic or Electronically Excited Gases, II. Jour. Chem. Phys., vol. 26, no. 2, Feb. 1957, pp. 282-285.

18. Brokaw, Richard S.: Correlation of Turbulent Heat Transfer in a Tube for the Dissociating System $N_2O_4 \rightleftharpoons 2NO_2$. NACA RM E57K19a, 1958.

TABLE I. - COMPUTED THERMAL CONDUCTIVITIES[a] FOR THE $N_2O_4 \rightleftharpoons 2NO_2$ SYSTEM[b]

[Equilibrium thermal conductivity, $\lambda_e$; frozen thermal conductivity, $\lambda_f$: cal/(cm)(sec)(°K).]

| Temperature, °K | $\frac{DP}{RT}\frac{\Delta R^2}{RT^2}$, cal/(cm)(sec)(°K)(c) | Pressure, atm: 1.00 | | 0.74 | | 0.50 | | 0.33 | |
|---|---|---|---|---|---|---|---|---|---|
| | | $\lambda_e$ | $\lambda_f$ | $\lambda_e$ | $\lambda_f$ | $\lambda_e$ | $\lambda_f$ | $\lambda_e$ | $\lambda_f$ |
| 290 | $295.32\times10^{-5}$ | $20.083\times10^{-5}$ | $3.110\times10^{-5}$ | $22.332\times10^{-5}$ | $3.136\times10^{-5}$ | $25.506\times10^{-5}$ | $3.174\times10^{-5}$ | $29.106\times10^{-5}$ | $3.221\times10^{-5}$ |
| 300 | 285.28 | 25.668 | 3.337 | 28.201 | 3.373 | 31.523 | 3.425 | 34.829 | 3.488 |
| 310 | 275.43 | 31.176 | 3.587 | 33.498 | 3.633 | 36.075 | 3.700 | 37.844 | 3.776 |
| 320 | 266.38 | 35.233 | 3.860 | 36.578 | 3.916 | 37.288 | 3.992 | 36.481 | 4.072 |
| 330 | 257.80 | 36.366 | 4.143 | 36.073 | 4.203 | 34.404 | 4.278 | 31.189 | 4.352 |
| 340 | 249.42 | 33.977 | 4.427 | 32.025 | 4.482 | 28.504 | 4.549 | 24.217 | 4.608 |
| 350 | 241.45 | 29.086 | 4.693 | 26.197 | 4.740 | 22.170 | 4.792 | 18.109 | 4.835 |
| 360 | 234.10 | 23.308 | 4.938 | 20.304 | 4.975 | 16.747 | 5.012 | 13.554 | 5.042 |
| 370 | 226.93 | 18.037 | 5.163 | 15.542 | 5.188 | 12.805 | 5.214 | 10.557 | 5.234 |
| 380 | 220.16 | 14.087 | 5.368 | 12.201 | 5.384 | 10.262 | 5.401 | 8.752 | 5.414 |
| 390 | 213.73 | 11.262 | 5.561 | 9.939 | 5.573 | 8.650 | 5.585 | 7.663 | 5.593 |
| 400 | 207.45 | 9.478 | 5.745 | 8.576 | 5.753 | 7.717 | 5.761 | 7.078 | 5.766 |
| 410 | 201.40 | 8.375 | 5.925 | 7.769 | 5.929 | 7.196 | 5.934 | 6.781 | 5.937 |
| 420 | 195.72 | 7.742 | 6.098 | 7.331 | 6.102 | 6.946 | 6.105 | 6.667 | 6.108 |
| 430 | 190.24 | 7.397 | 6.272 | 7.114 | 6.275 | 6.849 | 6.277 | 6.657 | 6.279 |
| 440 | 185.03 | 7.219 | 6.446 | 7.024 | 6.448 | 6.840 | 6.450 | 6.711 | 6.451 |
| 450 | 180.06 | 7.143 | 6.617 | 7.008 | 6.618 | 6.885 | 6.619 | 6.796 | 6.620 |
| 460 | 175.09 | 7.163 | 6.791 | 7.069 | 6.792 | 6.980 | 6.793 | 6.918 | 6.794 |
| 470 | 170.50 | 7.223 | 6.958 | 7.154 | 6.959 | 7.092 | 6.960 | 7.048 | 6.960 |
| 480 | 166.03 | 7.315 | 7.127 | 7.267 | 7.128 | 7.222 | 7.128 | 7.191 | 7.129 |
| 490 | 161.69 | 7.436 | 7.300 | 7.401 | 7.300 | 7.369 | 7.300 | 7.346 | 7.301 |

| Temperature, °K | Pressure, atm: 0.20 | | 0.10 | | 0.05 | | 0.02 | |
|---|---|---|---|---|---|---|---|---|
| | $\lambda_e$ | $\lambda_f$ | $\lambda_e$ | $\lambda_f$ | $\lambda_e$ | $\lambda_f$ | $\lambda_e$ | $\lambda_f$ |
| 290 | $33.463\times10^{-5}$ | $3.289\times10^{-5}$ | $38.509\times10^{-5}$ | $3.401\times10^{-5}$ | $40.418\times10^{-5}$ | $3.529\times10^{-5}$ | $35.434\times10^{-5}$ | $3.697\times10^{-5}$ |
| 300 | 37.946 | 3.574 | 39.227 | 3.704 | 35.693 | 3.833 | 25.576 | 3.971 |
| 310 | 38.055 | 3.872 | 34.258 | 4.002 | 26.928 | 4.109 | 16.830 | 4.204 |
| 320 | 33.315 | 4.165 | 26.180 | 4.273 | 18.587 | 4.349 | 11.267 | 4.407 |
| 330 | 26.037 | 4.429 | 18.662 | 4.507 | 12.842 | 4.556 | 8.271 | 4.590 |
| 340 | 19.039 | 4.664 | 13.224 | 4.716 | 9.411 | 4.746 | 6.744 | 4.765 |
| 350 | 13.970 | 4.874 | 9.950 | 4.907 | 7.590 | 4.925 | 6.039 | 4.936 |
| 360 | 10.640 | 5.067 | 8.053 | 5.087 | 6.631 | 5.098 | 5.729 | 5.105 |
| 370 | 8.632 | 5.250 | 7.022 | 5.262 | 6.179 | 5.269 | 5.636 | 5.275 |
| 380 | 7.517 | 5.424 | 6.502 | 5.432 | 5.976 | 5.436 | 5.657 | 5.439 |
| 390 | 6.878 | 5.599 | 6.254 | 5.605 | 5.935 | 5.607 | 5.740 | 5.609 |
| 400 | 6.576 | 5.770 | 6.180 | 5.774 | 5.980 | 5.775 | 5.858 | 5.776 |
| 410 | 6.457 | 5.940 | 6.202 | 5.942 | 6.072 | 5.944 | 5.996 | 5.944 |
| 420 | 6.451 | 6.110 | 6.279 | 6.111 | 6.198 | 6.112 | 6.147 | 6.112 |
| 430 | 6.511 | 6.280 | ---------- | ---------- | ---------- | ---------- | ---------- | ---------- |
| 440 | 6.610 | 6.452 | ---------- | ---------- | ---------- | ---------- | ---------- | ---------- |
| 450 | 6.728 | 6.621 | ---------- | ---------- | ---------- | ---------- | ---------- | ---------- |
| 460 | 6.869 | 6.794 | ---------- | ---------- | ---------- | ---------- | ---------- | ---------- |
| 470 | 7.014 | 6.960 | ---------- | ---------- | ---------- | ---------- | ---------- | ---------- |
| 480 | 7.166 | 7.129 | ---------- | ---------- | ---------- | ---------- | ---------- | ---------- |
| 490 | 7.328 | 7.301 | ---------- | ---------- | ---------- | ---------- | ---------- | ---------- |

[a]Effects of $NO_2$ dissociation, which may be of major significance above 400° K, have not been included.
[b]Viscosity, density, and specific heat are tabulated for 1.00, 0.74, and 0.33 atmospheres in ref. 18.
[c]From eq. (6) and p. 9 in text.

(a) Block assembly.




(b) Internal cell construction.

Figure 1. - Thermal conductivity cells.

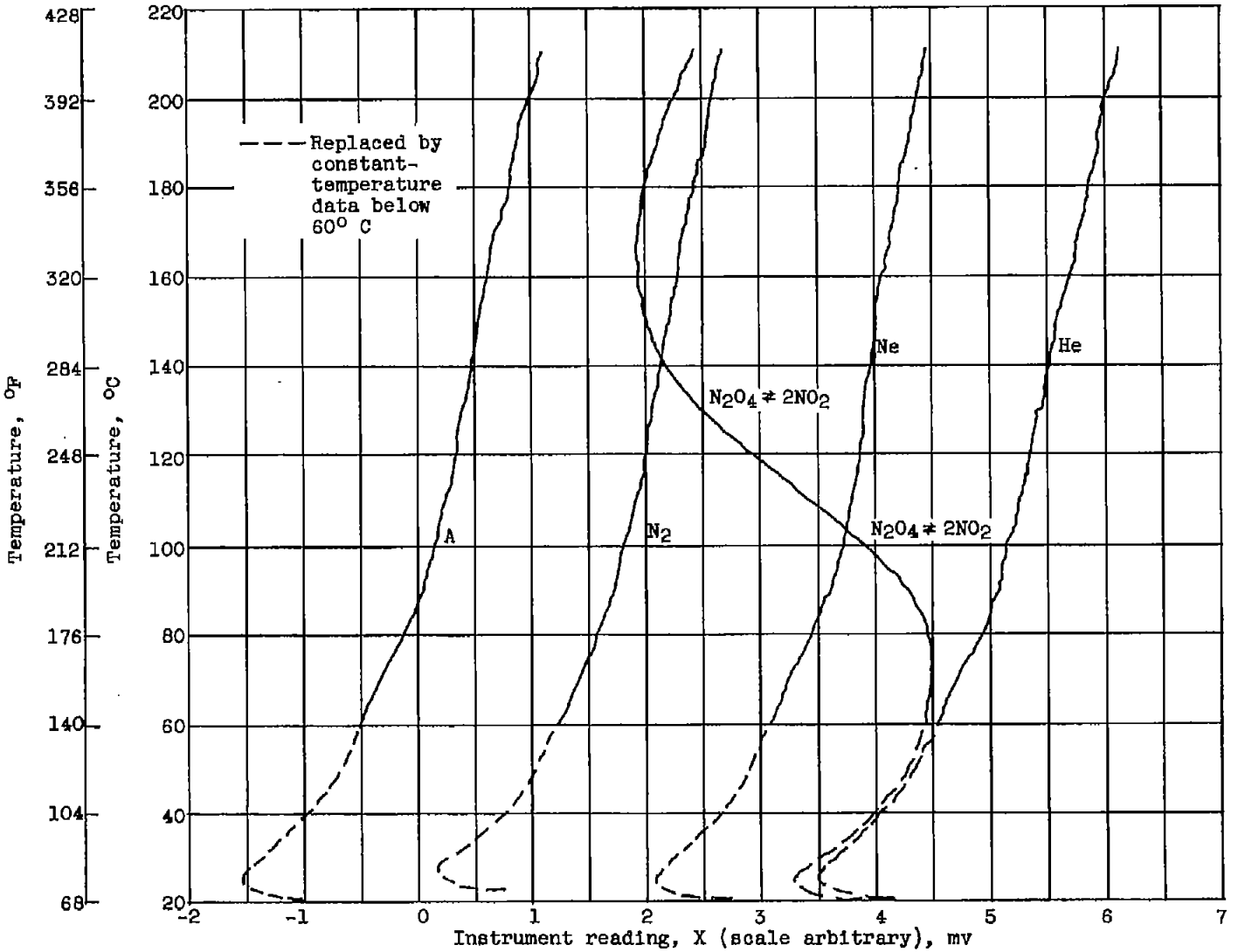


Figure 2. - Instrument traces taken at 1 atmosphere.

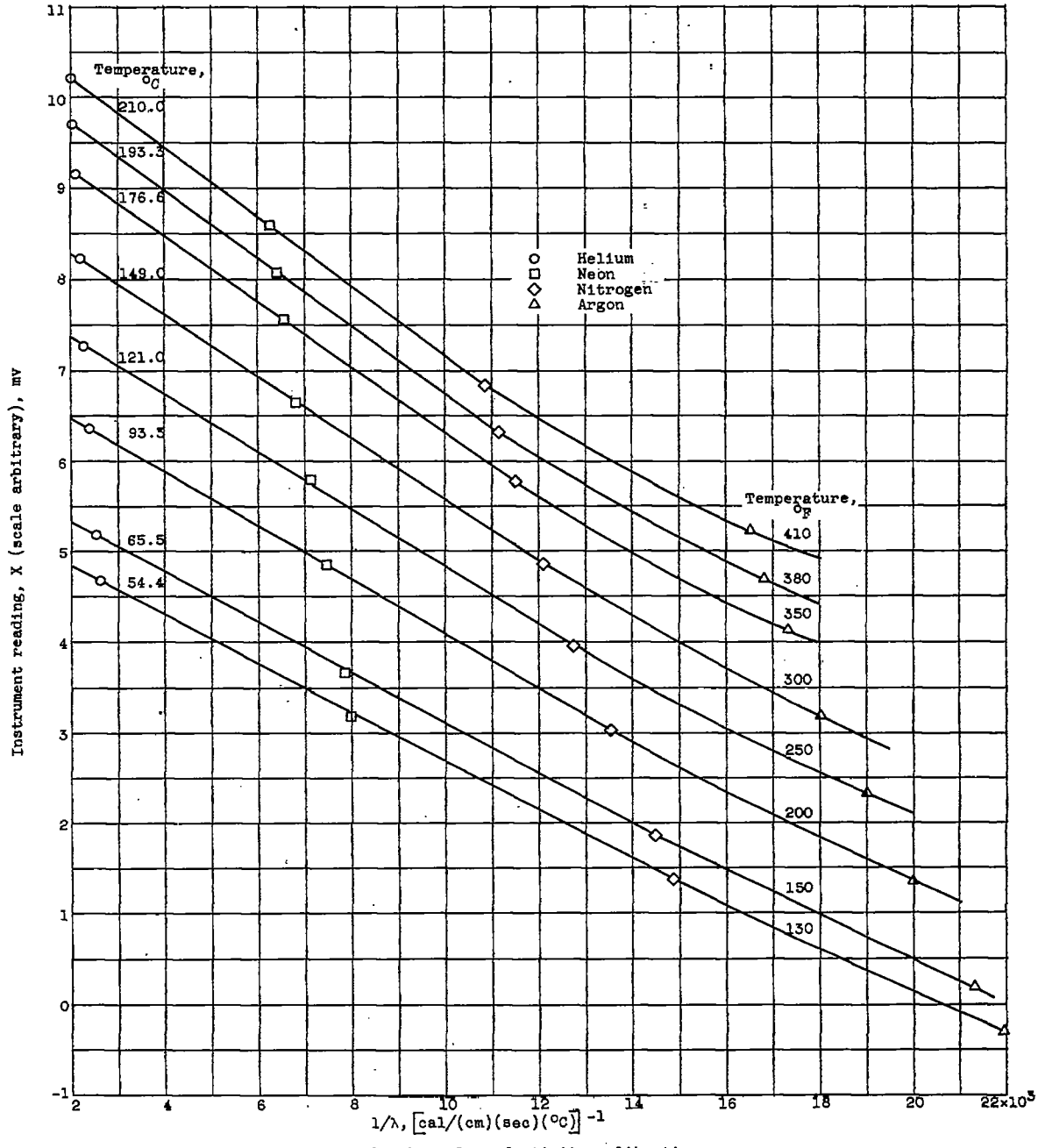


Figure 3. - Sample thermal-conductivity calibration curves.

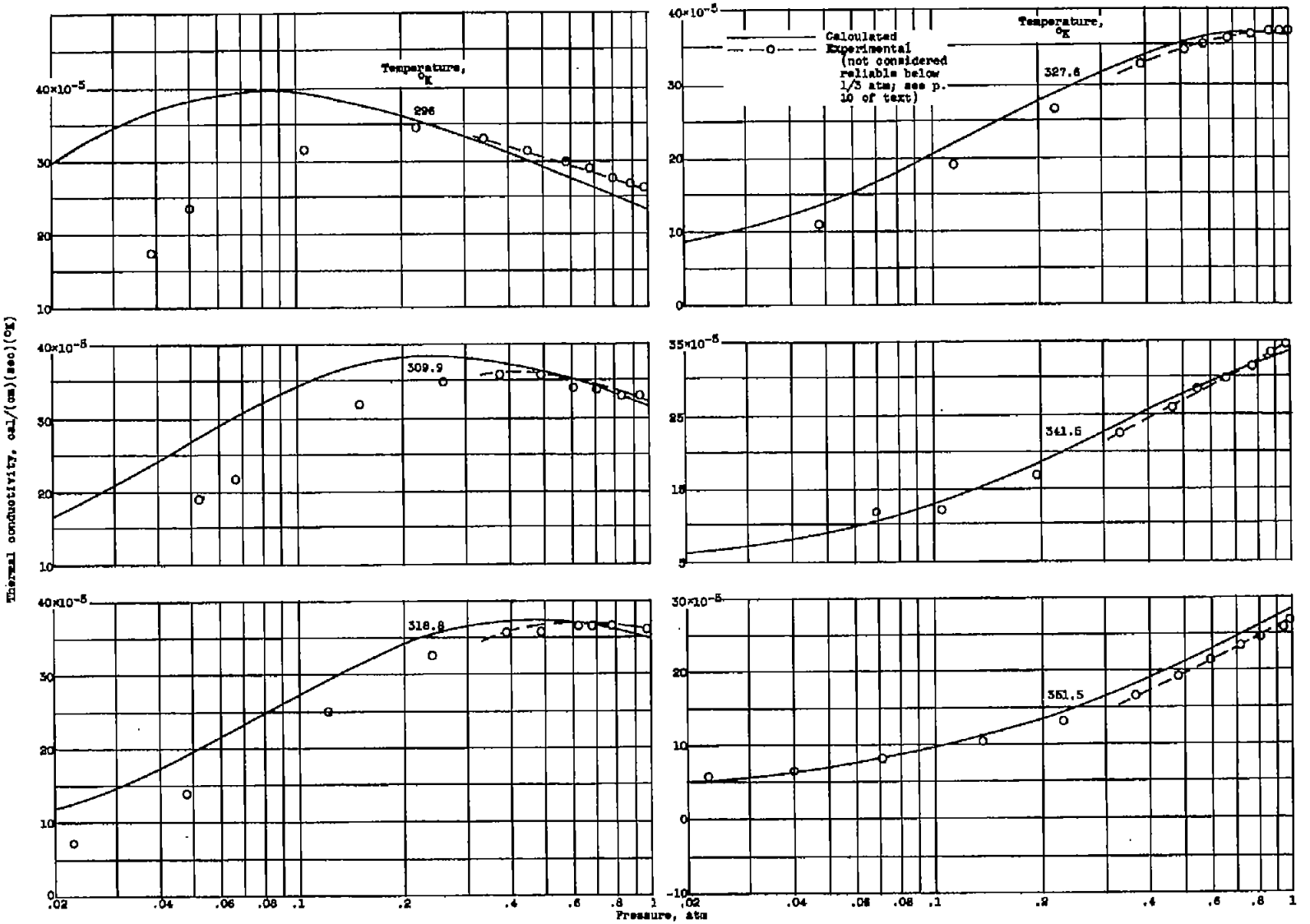


Figure 4. - Effect of pressure on thermal conductivity of $N_2O_4 \rightleftharpoons 2NO_2$ system.

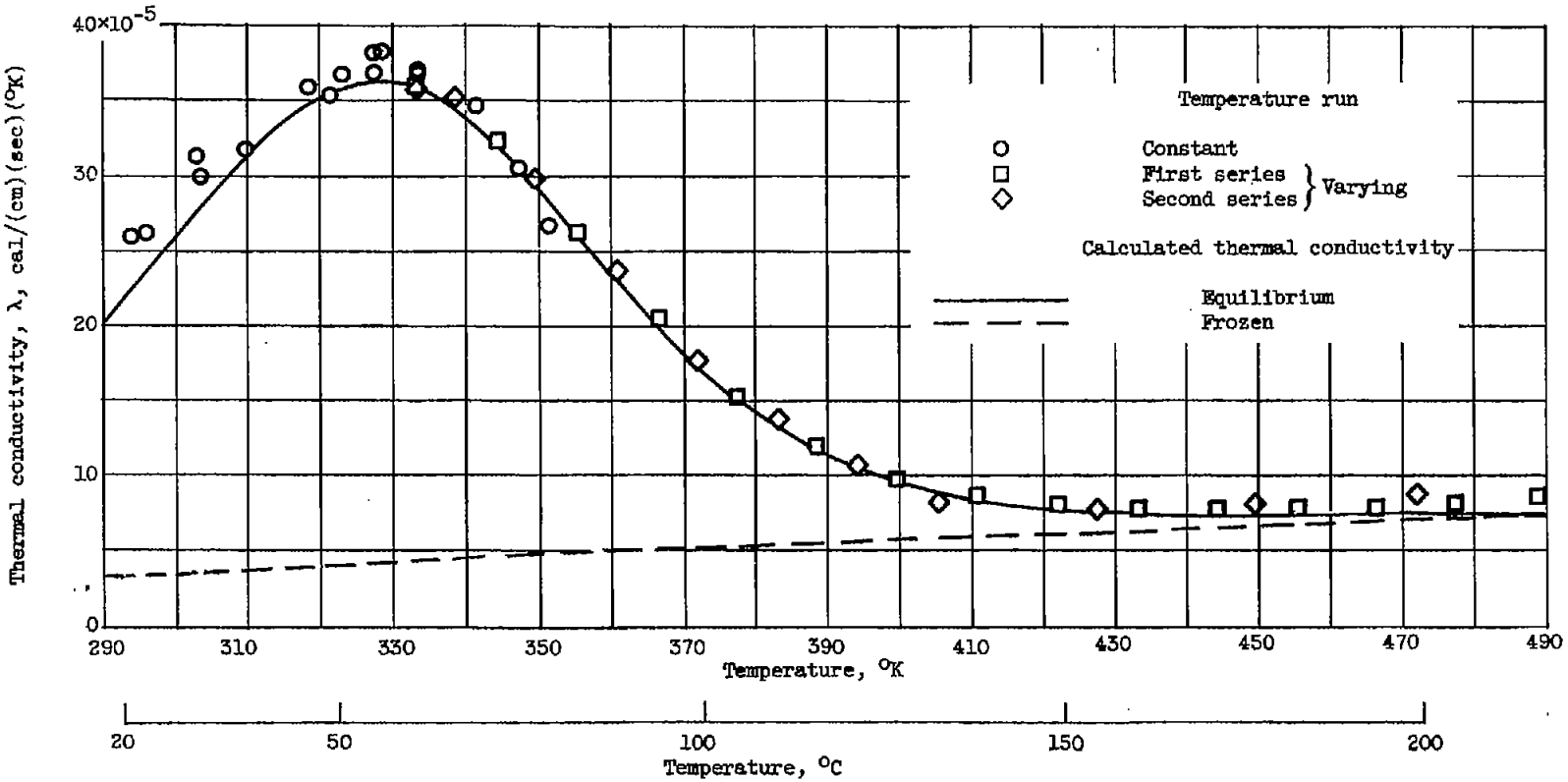


(a) Pressure, 1 atmosphere.

Figure 5. - Thermal conductivity of dissociating $N_2O_4$.

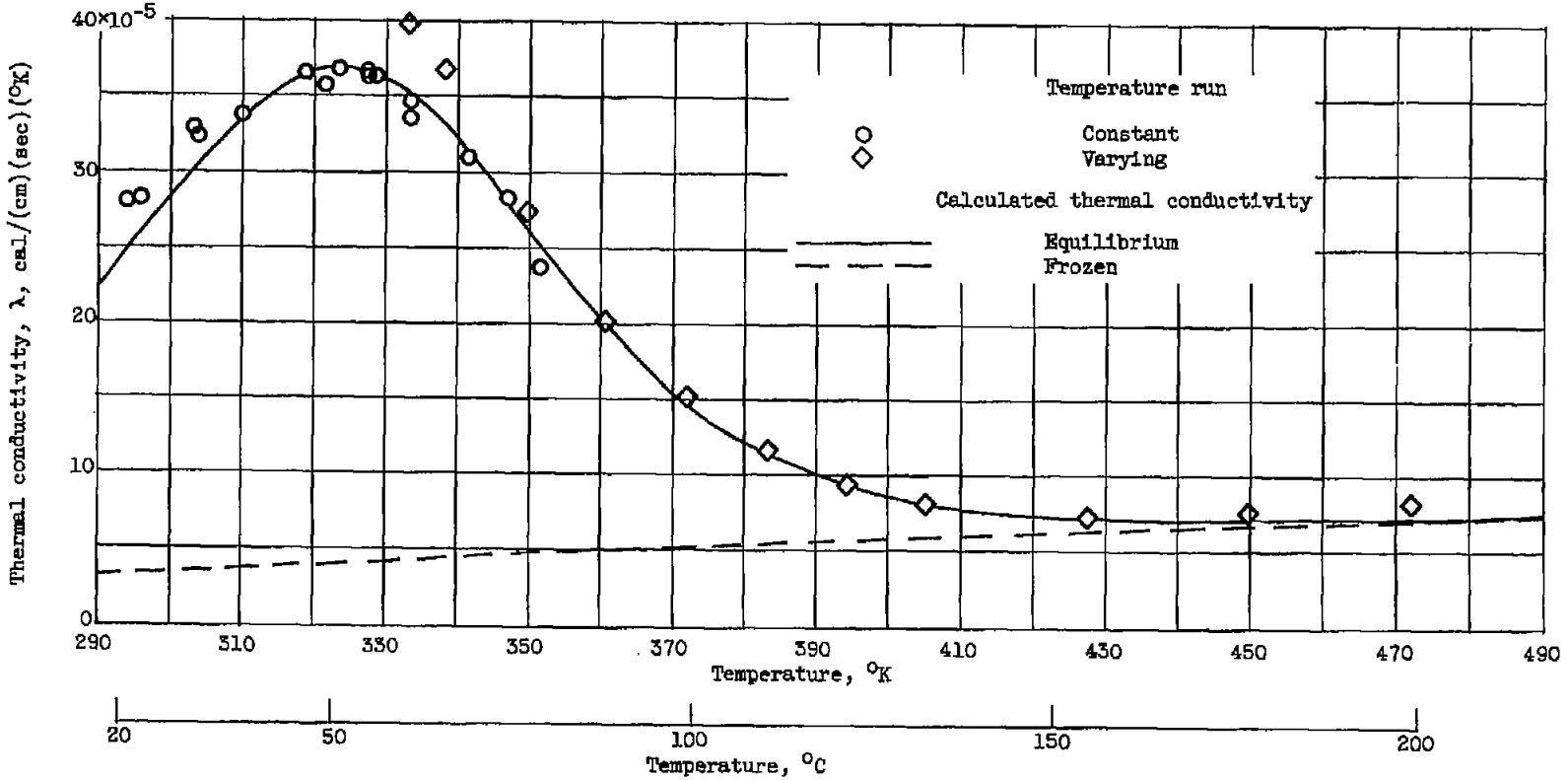


(b) Pressure, 0.74 atmosphere.

Figure 5. - Continued. Thermal conductivity of dissociating $N_2O_4$.

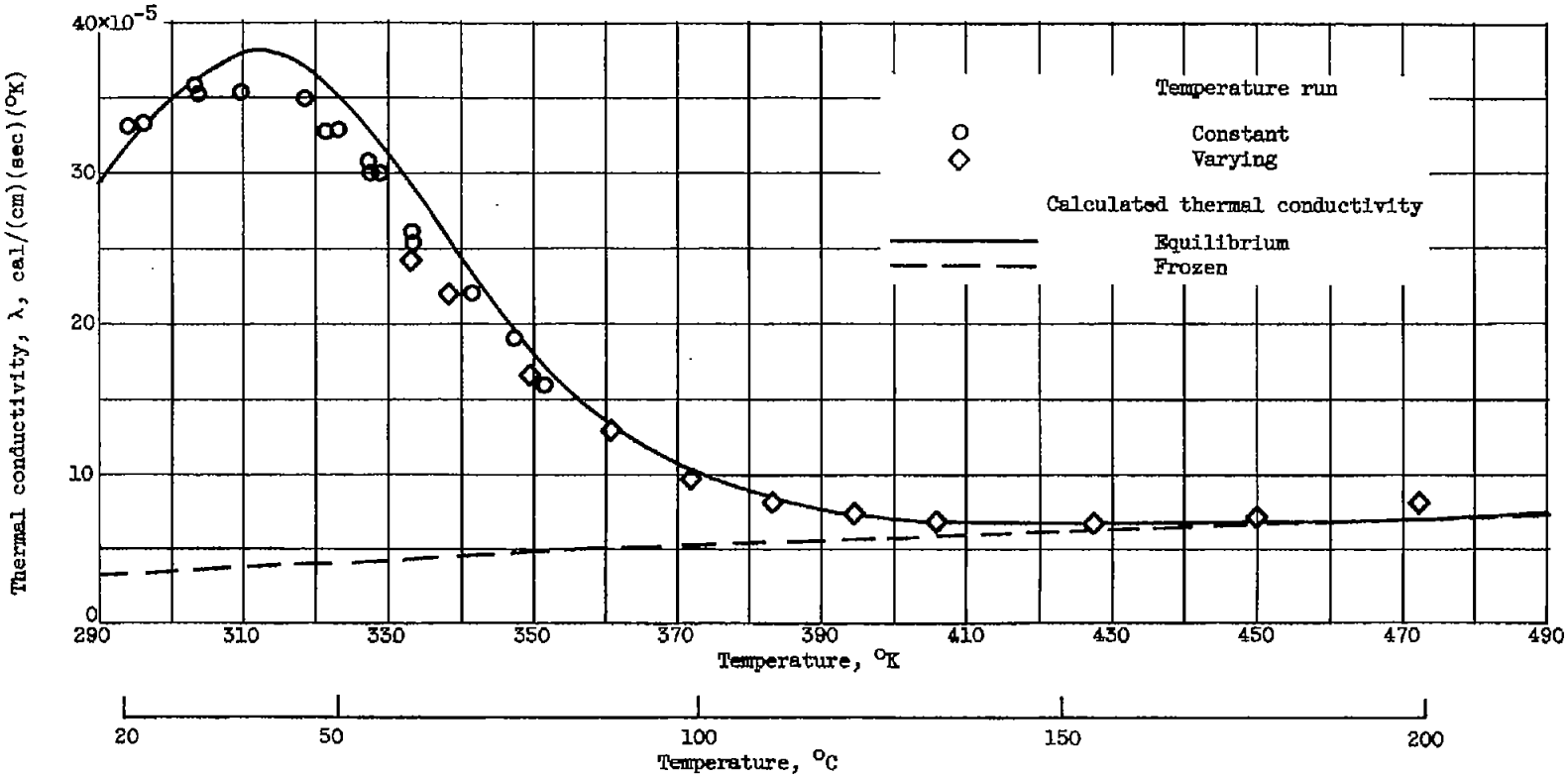


(c) Pressure, 0.33 atmosphere.

Figure 5. - Concluded. Thermal conductivity of dissociating $N_2O_4$.